Hindawi
International Journal of Photoenergy
Volume 2018, Article ID 5290975, 9 pages
https://doi.org/10.1155/2018/5290975

Research Article

A Comparative Analysis of 2-(Thiocyanomethylthio)-Benzothiazole Degradation Using Electro-Fenton and Anodic Oxidation on a Boron-Doped Diamond Electrode

Armando Vázquez,[1] Lucía Alvarado,[2] Isabel Lázaro,[1] Roel Cruz,[1] José Luis Nava,[3] and Israel Rodríguez-Torres[1]

[1]*Instituto de Metalurgia, Facultad de Ingeniería, Universidad Autónoma de San Luis Potosí, Av. Sierra Leona 550, 78210 San Luis Potosí, SLP, Mexico*
[2]*Departamento de Ingeniería en Minas, Metalurgia y Geología, Universidad de Guanajuato, Ex. Hacienda de San Matías s/n Fracc. San Javier, 36025 Guanajuato, GTO, Mexico*
[3]*Departamento de Ingeniería Geomática e Hidráulica, Universidad de Guanajuato, Av. Juárez 77, 36000 Guanajuato, GTO, Mexico*

Correspondence should be addressed to Israel Rodríguez-Torres; learsi@uaslp.mx

Received 18 October 2017; Accepted 3 January 2018; Published 1 March 2018

Academic Editor: Reyna Natividad-Rangel

2-(Thiocyanomethylthio)-benzothiazole (TCMTB) is used as fungicide in the paper, tannery, paint, and coatings industries, and its study is important as it is considered toxic to aquatic life. In this study, a comparison of direct anodic oxidation (AO) using a boron-doped diamond electrode (BDD) and electro-Fenton (EF) processes for TCMTB degradation in acidic chloride and sulfate media using a FM01-LC reactor was performed. The results of the electrolysis processes studied in the FM01-LC reactor showed a higher degradation of TCMTB with the anodic oxidation process than with the electro-Fenton process, reaching 81% degradation for the former process versus 47% degradation for the latter process. This difference was attributed to the decrease in H_2O_2 during the EF process, due to parallel oxidation of chlorides. The degradation rate and current efficiency increased as a function of volumetric flow rate, indicating that convection promotes anodic oxidation and electro-Fenton processes. The results showed that both AO and EF processes could be useful strategies for TCMTB toxicity reduction in wastewaters.

1. Introduction

The paper industry has been identified as a major source of pollutants to aquatic environments due to the large volume of wastewater generated per ton of paper produced. The effluents generated during the paper production process cause damage to the receiving waters as they contain high levels of total organic carbon (TOC) and exhibit a chemical oxygen demand (COD) above the permissible limits [1]. Studies on the treatments of wastewater from the paper industry have reported a content of at least 300 different compounds, including certain compounds of biocide nature [2], such as 2-(thiocyanomethylthio)-benzothiazole (TCMTB), which is often used as a biocide in the wood [3] and tannery industries [4]. TCMTB is listed as hazardous by the Environmental Protection Agency of the United States, and it is considered highly toxic to freshwater fish, freshwater invertebrates, estuarine/marine fish, and estuarine/marine invertebrates [5]. Hence, it is important to develop and apply techniques for the degradation of TCMTB.

Reemtsma et al. [6] achieved an incomplete TCMTB degradation (75%) in an anaerobic and aerobic wastewater treatment pilot plant, yielding mercaptobenzothiazole (MTB), benzothiazole (BT), and hydroxybenzotriazole (OHBT) as the degradation products, which however are harmful compounds that cause dermatitis [7], cell apoptosis [8], and respiratory tract irritation [9], respectively. De Wever et al. [10, 11] carried out studies to investigate the biodegradation of these compounds and established that MTB is a recalcitrant compound. Recalcitrant compounds or persistent

organic pollutants (POPs) are characterized by a high stability against sunlight irradiation and a high resistance to either microbial attack (biological processes) or temperature.

Advanced oxidation processes (AOPs) are effective methods that have been developed for POP treatment. These methods primarily involve hydrogen peroxide, ozone, UV-near visible light in the presence of TiO_2, the Fenton reagent, sonolysis, and the sulfate radical-based AOP [12]. Advanced electrooxidation processes (AEOPs) have been proposed as alternative methods for the removal of organics; these processes employ electrochemical cells in which oxidants are produced in situ on the electrode surface [13].

In recent years, the development of AEOPs has significantly increased, particularly oriented to processes of POP degradation. AEOPs are based on the generation of strong oxidizing species, such as the hydroxyl radical ($^{\cdot}OH$), which can alter the chemical structure of the contaminants [14]. The hydroxyl radical is considered the most important free radical in chemistry due to its strong oxidizing nature ($E^{\circ} = 2.8$ V), which is exceeded only by fluorine ($E^{\circ} = 3.05$ V). The oxidizing power of $^{\cdot}OH$ destroys most organic pollutants until total mineralization is achieved, that is, conversion to CO_2, water, and inorganic ions.

In this context, one method of generating the hydroxyl radical is through the Fenton reaction. The Fenton process mechanism is initiated by the formation of the homogeneous hydroxyl radical in accordance with the classical Fenton reaction in acidic medium, as follows [14]:

$$Fe^{2+} + H_2O_2 + H^+ \rightarrow Fe^{3+} + H_2O + {}^{\cdot}OH \quad (1)$$

This technique becomes an attractive choice because only a small catalytic amount of Fe^{2+} is required during the entire process due to the continuous regeneration of the ion from the Fenton-like reaction [15].

Another interesting aspect of $^{\cdot}OH$ production from H_2O_2 is that it can be generated by electrochemical reduction from O_2 in aqueous solution under acidic conditions, as follows [14, 16]:

$$O_2 + 2H^+ + 2e^- \rightarrow H_2O_2 \quad (2)$$

Electro-Fenton (EF) technology is based on the continuous electrogeneration of H_2O_2 on a suitable cathode (generally, carbon-based), which is fed with either O_2 or air [14], and the addition of an iron catalyst to produce the oxidant hydroxyl radical at the bulk via the Fenton reaction, according to (1).

Another electrochemical process that could generate $^{\cdot}OH$ radicals is the anodic oxidation of water [17–19]:

$$H_2O + BDD \rightarrow ({}^{\cdot}OH)BDD + H^+ + e^- \quad (3)$$

Hydroxyl radical formation is favored on boron-doped diamond (BDD) thin film anodes; this reaction is based on the use of high O_2 overvoltage anodes favoring heterogeneous hydroxyl radical production, BDD($^{\cdot}OH$). It has been reported that organic compounds can be destroyed by anodic oxidation using BDD electrodes, resulting in their complete mineralization [20].

This study compares TCMTB degradation via the electro-Fenton (EF) process and the anodic oxidation process in a filter press reactor FM01-LC. For the EF process, a reticulated vitreous carbon was used as the cathode along with a dimensionally stable anode (DSA) made of Ti with a cover of IrO_2/Ta_2O_5; for the AO process, a BDD electrode was used as anode, and a stainless steel electrode was used as cathode.

2. Materials and Methods

2.1. Reagents and Physicochemical Analysis. All of the chemicals used were of analytical grade, and deionized water (18 MΩ cm) was employed for the preparation of solutions. The organic compound TCMTB was purchased from Insumos Agrícolas Company (industrial grade, 30% purity). The pH measurements were obtained using a Thermo Orion pH meter 420A. The H_2O_2 concentration was determined using the $Ti(SO_4)_2$ colorimetric method and analyzed by UV-vis spectrophotometry at $\lambda = 410$ nm[21]. The performance of the process was evaluated following TCMTB UV-vis absorbance at $\lambda = 290$ nm [3] in a Shimadzu UV/VIS/NIR spectrophotometer UV-3600 with a scanning stage step of 250 nm. Total organic carbon (TOC) was measured with a Shimadzu total organic carbon analyzer 5000A, and chemical oxygen demand (COD) tests were run according to standard protocols [22].

2.2. Microelectrolysis

2.2.1. Experimental Devices. A three-electrode system was used for voltammetric experiments using a 100 mL Pyrex electrochemical cell. The potential was applied using a Princeton Applied Research potentiostat-galvanostat VersaSTAT, and Versa software was used to record the data. For the AO study, a BDD rotating disc electrode (RDE) with a surface area of 0.03141 cm^2 and a DSA (Ti with a cover of IrO_2/Ta_2O_5) with a surface area of 0.096 cm^2 were used as working electrodes. For the cathodic production of hydrogen peroxide, RDE made of vitreous carbon and stainless steel 304 were used, both with a surface area of 0.196 cm^2. The BDD was cleaned using an anodic polarization treatment (1 M $HClO_4$) for 30 min at 10 mA cm^{-2} [23].

A graphite rod was used as the counter electrode in both sets of experiments. Potential measurements were obtained versus a saturated mercurous sulfate reference electrode (SSE) with a potential of 0.6415 V. All the potential measurements shown in this study were referred to the standard hydrogen electrode (SHE). To ensure reproducibility, all of the experiments were performed in triplicate.

2.2.2. Voltammetric Studies. To determine the best current density and electrode potential domain to be applied to favor both the electro-Fenton process (cathodic H_2O_2) and the anodic oxidation (anodic $^{\cdot}OH$), a microelectrolysis study was performed. For this study, two types of solutions were used: (a) a blank solution (0.02 M NaCl and 0.03 M Na_2SO_4) and (b) a synthetic solution (0.02 M NaCl, 0.03 M Na_2SO_4, and 0.07 M TCMTB). The concentration of the blank solution was fixed to an ionic strength similar to that registered in wastewater from the paper industry [24]. The TCMTB

concentration was set to achieve a 570 mg L^{-1} TOC (similar to the concentration found in paper industry effluents), which is equivalent for a turbidity of approximately 383 NTU (nephelometric turbidity unit).

Prior to starting the EF experiments, each solution was aerated for 60 min to insure O_2 saturation and acidified with 1 M H_2SO_4 to reach a pH of 3.

A series of anodic and cathodic potential pulses were applied on static electrodes for 30 s from the open-circuit potential (OCP) to positive potentials for the anodic process and to negative potentials for the cathodic process. From the current transients obtained, j-E curves were constructed using current density data sampled at different times for each potential applied.

2.3. Macroelectrolysis

2.3.1. Experimental Devices. Macroelectrolysis experiments were performed in an FM01-LC electrochemical reactor [25, 26]. Figure 1(a) shows an expanded view, including the turbulence promoter type D [27]. The flow distributor thickness was 0.6 cm; a stainless steel plate (64 cm^2 exposed area) and reticulated vitreous carbon (RVC) of 16 × 4 cm and 0.4 cm of thickness (10 pores per inch (ppi), porosity of 0.99, and specific surface area of 4.92 cm^{-1}) were used as cathodes, and BDD and DSA plates (64 cm^2) were used as anodes. The volume of electrolyte to fill the reactor was 28.2 cm^3. A mercury/mercurous sulfate reference electrode Hg/Hg_2SO_4 was connected to the electrochemical reactor to measure the electrode potential. More details of the FM01-LC are described in detail in [25].

An undivided mode configuration with a single electrolyte compartment and electrolyte flow circuit for the FM01-LC cell is shown in Figure 1(b). The electrolyte was contained in a 2.5 L acrylic reservoir; a Marathon Electric™ 1/3 HP centrifugal coupled pump 335AD-MD was used, and flow rates were measured by a Cole-Parmer variable area plastic flow meter F44500. The electrolyte flow circuit was constructed using 0.5-inch internal diameter PVC tubing and valves as well as three-way connectors constructed of the same material. The experiments were conducted using a Sorensen high-power DC power supplies. In experiments to evaluate H_2O_2 production, the electrochemical reactor was fitted with a RVC as cathode and a stainless steel electrode as anode. For the EF process, the reactor was equipped with the RVC as cathode and DSA as anode; for the AO method, a stainless steel electrode as cathode and a BDD as anode were used.

2.3.2. Electrochemical Degradation of TCMTB in a FM01-LC Filter Press-Type Electrochemical Cell. All of the experiments in the FM01-LC cell were performed at three different volumetric flows (Q_v): 5.67, 9.46, and 13.24 L min^{-1}. For each experiment, the final TOC values were measured, and the integral current efficiency was calculated using [25]

$$\phi = \frac{4FV\left[\mathrm{TOC}_{(0)} - \mathrm{TOC}_{(t)}\right]}{IT}, \quad (4)$$

where F is the Faraday constant with a value of 96,485 C mol^{-1}, V is the solution volume (L), I is the current applied (A), and t is the time of electrolysis (s), which for these experiments was 180 minutes.

For electro-Fenton experiments, H_2O_2 generation was achieved using RVC as the cathode, DSA as the anode, and a blank solution as the electrolyte applying a constant current density. This value was determined by varying the current density until reaching the electrode potential determined by the microelectrolysis experiments, which was within $-1.15 \le E \le -0.95$ V/SHE. The RVC cathode was supported on a stainless steel plate (current feeder) using conductive carbon paint glue (SPI supplies™).

Prior to starting the EF experiments, each solution was aerated for 60 min to be saturated with O_2 and acidified with 1 M H_2SO_4 to reach a pH of 3. As an initial step, the concentration of H_2O_2 generated in the blank solution was monitored. For the case of H_2O_2 production in the synthetic solution (in presence of TCMTB), it was not possible to measure its concentration using the colorimetric method because the organic compound caused interference. To determine the current density to be applied to the synthetic solution, the same methodology was used; subsequently, the Fenton reaction was promoted by the addition of 0.5 mM Fe^{2+}, which is a similar concentration to that reported by other studies Peralta et al. [15] and Pérez et al. [28], where it was shown mineralization percentages of around 50%.

For the anodic oxidation tests, a BDD was used as the anode and a stainless steel plate was used as the cathode, applying a constant current density that enabled control of the potential at the anode to obtain ($^{\cdot}$OH)BDD.

3. Results and Discussion

3.1. Microelectrolysis Studies of the Electro-Fenton Process. Typical sampled current density (j-E) curves constructed from current density transients (not shown) are illustrated in Figure 2. The j-E curves were obtained at different constant potential pulses and sampling times from 1 to 30 s, using a vitreous carbon electrode for both the blank solution (continuous lines) and the synthetic solution (semi-continuous and dashed lines).

The curves for the blank solution exhibit three electrochemical processes: Ia electrochemical generation of H_2O_2 from −0.95 to −1.15 V/SHE, (2); IIa electrochemical generation of water from −1.35 to −1.5 V/SHE, (5); and IIIa water reduction below −1.65 V/SHE, (6).

$$O_2 + 4H^+ + 4e^- \rightarrow 2H_2O \quad (5)$$

$$2H_2O + 2e^- \rightarrow H_2 + 2OH^- \quad (6)$$

When the organic compound was added (semi-continuous and dashed lines), a new process Ib is observed at potentials from −0.33 to −0.66 V/SHE, which is related to TMCTB but it does not seem to depend on concentration. Then, a similar Ia process is observed at the same potential region observed for the blank solution (−0.95 to −1.15 V); however, TCMTB seems to favor the electrochemical production of H_2O_2 given that the current density is enhanced as the concentration of this organic compound is increased (from 0.035 to 0.07 M). At potentials around −1.36 V/SHE, the

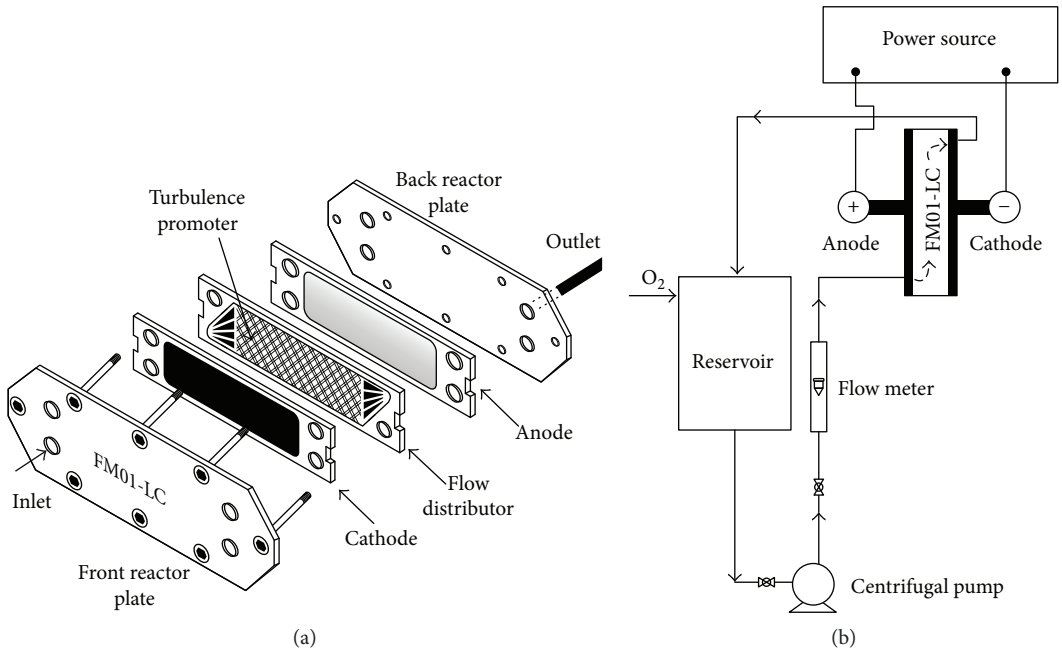

Figure 1: (a) Expanded view of the FM01-LC cell in the undivided mode. (b) Electrical and flow circuits for the electrochemical flow experiments.

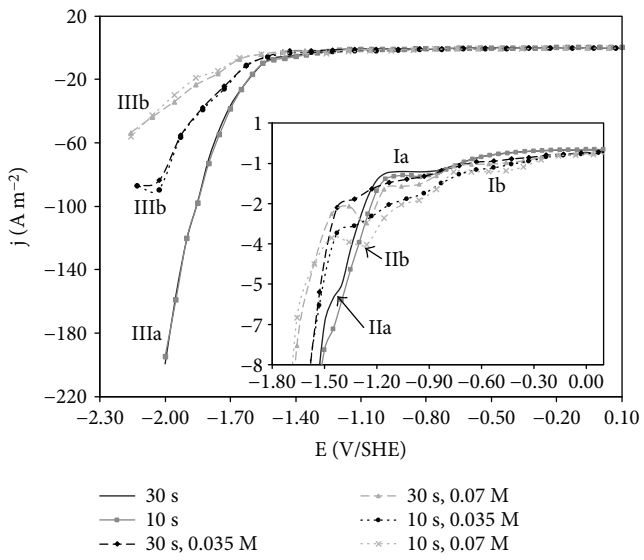

Figure 2: Typical j-E curves obtained by sampling current density at different times from current transients obtained at potential pulses between $-2\,V < E > 0.1\,V$ using a vitreous carbon RDE in a blank solution (NaCl 0.02 M and Na_2SO_4 0.03 M, pH 3; continuous lines) and in a synthetic solution (0.02 M NaCl and 0.03 M Na_2SO_4, pH 3, 0.07 M TCMTB—semi-continuous lines; 0.035 M TCMTB—dashed lines). The inset shows an enhanced view. $A_{RDE} = 0.196\,cm^2$.

observed peak (IIb) corresponds to a two-electron reduction process by molecule of TCMTB as reported [4].

Likewise, the reduction of water is shifted to more negative potentials (IIIb), as TCMTB concentration is increased. It is observed that for the two types of solutions, with and without TCMTB, the current density for all of the processes decreases as the sampling time increases, indicating a mass transport limitation. Moreover, in Figure 2, current density plateaus appeared for the process Ia, which decreased relative to the sampling time, indicating that this process (electrochemical production of H_2O_2) is limited by diffusion.

The anodic processes on the DSA electrode in the blank solution and the synthetic solution were evaluated (Figure 3), and the obtained curves showed that in both solutions, the oxidation becomes important at potentials above 1.4 V/SHE. The low currents obtained in the presence of TCMTB, with respect to blank solution, suggest that in addition to the oxidation processes, part of the energy is also being used for the possible oxidation of the compound. Thus, the oxidation process in the synthetic solution might include the oxidation of hydrogen peroxide, chloride to produce active chlorine, TCMTB with anodically electrogenerated species, and the OER (oxygen evolution reaction); therefore, a careful potential control during the process becomes important [29, 30].

3.2. Microelectrolysis Studies of Anodic Oxidation on the BDD Electrode. A voltammetric study of the cathodic reactions on stainless steel shows only the reduction of the medium from −1.5 V/SHE for both solutions (Figure 4). No sign of TCMTB reduction was observed. A comparison of the results obtained for the synthetic solution on vitreous carbon (Figure 2) and on stainless steel (Figure 4) revealed that the reduction of water in the first case occurred at more negative potentials. This result indicates that the use of stainless steel as a cathode for this system could decrease the cell potential.

Figure 5 shows the curves of current density versus anodic potential pulse on the BDD in different solutions: (a) 1 M $HClO_4$, (b) blank solution, and (c) synthetic solution. In addition, Figure 5 shows a Tafel plot for the $HClO_4$ media, revealing that the current density increases as a function of

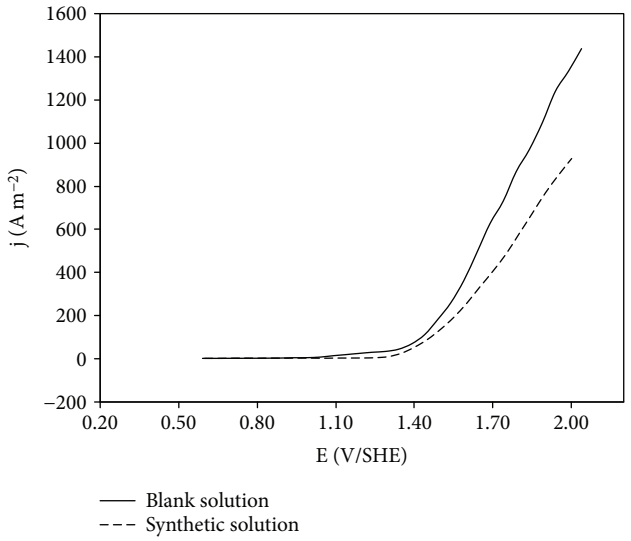

Figure 3: Typical j-E curves obtained by sampling current density at different times from typical current transients obtained at potential pulses between 0.5 V < E > 2 V using a DSA electrode in a blank solution (NaCl 0.02 M and Na_2SO_4 0.03 M, pH 3; continuous lines) and in a synthetic solution (0.07 M TCMTB, 0.02 M NaCl and 0.03 M Na_2SO_4, pH 3; dashed lines). $A_{RDE} = 0.09621\ cm^2$.

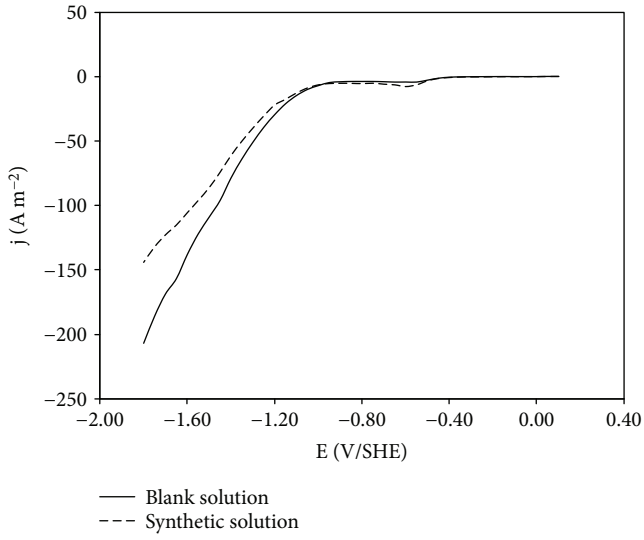

Figure 4: Typical j-E curves obtained by sampling current density at different times from typical current transients obtained at potential pulses between −1.8 V < E > 0.1 V using a stainless steel electrode in a blank solution (NaCl 0.02 M and Na_2SO_4 0.03 M, pH 3; continuous lines) and in a synthetic solution (0.07 M TCMTB, 0.02 M NaCl, and 0.03 M Na_2SO_4, pH 3; dashed lines). $A_{RDE} = 0.196\ cm^2$.

the imposed potential, which shows that detection of the faradaic current began above 2.3 V, which is consistent with the response of the BDD because this type of electrode requires higher overpotentials to oxidize water [25].

The Tafel slope from Figure 5(a) (insert) was evaluated over a potential range of $2.3 \le E \le 2.75$ V/SHE, and a value of 290 mV decade^{-1} was observed, which was similar to that reported by Michaud et al. [17], who determined a value of

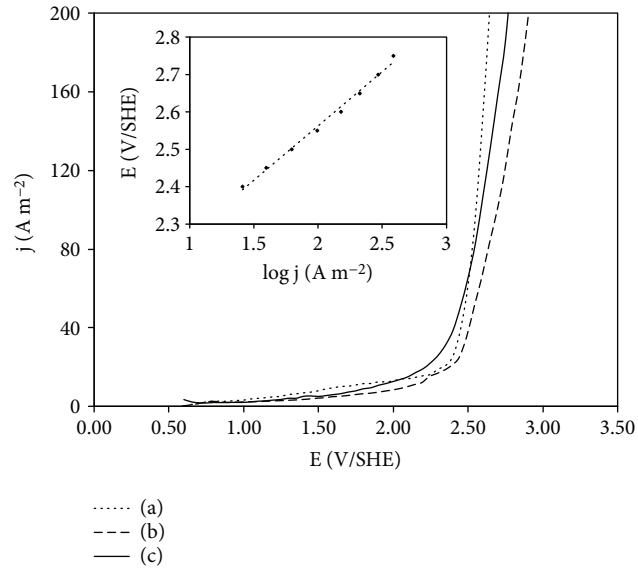

Figure 5: Typical j-E curves obtained by sampling current density at different times from typical current transients obtained at potential pulses between 0.6 V < E > 3 V using a BDD RDE for (a) 1 M $HClO_4$, (b) 0.02 M NaCl and 0.03 M Na_2SO_4 at pH 3, and (c) 0.07 M TCMTB in 0.02 M NaCl and 0.03 M Na_2SO_4 at pH 3. The inset shows the Tafel plot for j-E curves in (a). $A_{RDE} = 0.031416\ cm^2$.

250 mV decade^{-1} over a potential range of $2.4 \le E \le 2.9$ V/SHE in which the water oxidation was a one-electron process and the hydroxyl radical formation occurred according to (3). An analysis of the Tafel slopes over the potential range of $2.3 \le E \le 2.6$ V for the curves in Figures 5(b) and 5(c) (not shown) exhibited similar values in all cases. In addition, a certain amount of TCMTB adsorption on the BDD surface could be present in Figure 5(c), as indicated by the decrease in the current density. However, TCMTB would be oxidized through ($^{\cdot}$OH)BDD over the interval of $2.3 \le E \le 2.75$ V/SHE in addition to the active chlorine produced on the BDD surface, which will be discussed later.

3.3. Comparison between the Electrochemical Degradation of TCMTB by Electro-Fenton and by Anodic Oxidation on a BDD. A 2.4 mA cm^{-2} cathodic current density was applied to the RVC in the FM01-LC reactor to maintain the electrode potential over the range of $-0.95 \le E \le -1.15$ V/SHE and to promote the electrochemical generation of H_2O_2 on the RVC in the blank solution. As it is shown in Figure 6, the H_2O_2 concentration increases linearly with the volumetric flow rate over the first 30 min, and then it decreases for a short time; this behavior is repeated. This result is attributed to the instability of the H_2O_2 molecule, which is accompanied by its exothermic decomposition to oxygen and water, as follows [31]:

$$2H_2O_2 \rightarrow O_2 + 2H_2O \quad (7)$$

At room temperature (ca. 23°C), the rate of decomposition is slow; however, as the temperature increases, the rate of decomposition also increases [32]; in this study, the batch mode employed provoked a temperature solution of 60°C,

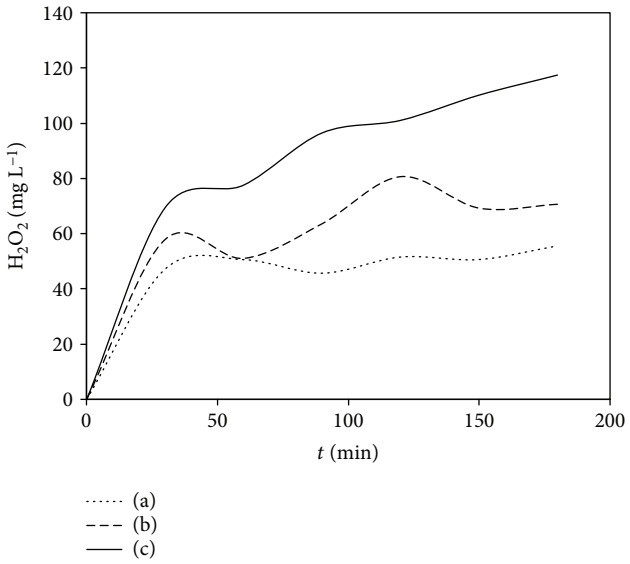

Figure 6: Influence of the volumetric flow rate on electrochemical generation of H_2O_2 on the RVC cathode fitted in the FM01-LC reactor. Electrolyte: 0.02 M NaCl and 0.03 M Na_2SO_4 at pH 3. $A_{RVC} = 125.95\ cm^2$, $A_{stainless\ steel} = 64\ cm^2$. 2.4 mA cm^{-2}. (a) 5.67 L min^{-1}, (b) 9.46 L min^{-1}, and (c) 13.24 L min^{-1}.

because of fluid recirculation. In addition, hydrogen peroxide could react with the chloride ions in solution [30], resulting in the formation of chlorine gas and water (8), which would explain the 8% decrease in the chloride concentration in all of the experiments using the blank solution.

$$H_2O_2 + 2Cl^- + 2H^+ \rightarrow 2H_2O + Cl_2 \quad (8)$$

Similar to other studies [33], the results obtained in this work showed that there is a mass transport limitation during cathodic H_2O_2 production, which decreases its concentration. However, as it has been reported even with the lowest H_2O_2 concentration (45 mg L^{-1}, $Q_v = 5.6$ L min^{-1}) achieved, it is possible to get an adequate Fenton reaction performance [31].

The current efficiency obtained for the electrochemical generation of H_2O_2 in RVC is shown in Table 1, demonstrating that the current efficiency increases as the volumetric flow increases. This result is attributed to the decrease in the resistance to mass transfer because the convection process is favored.

For the electro-Fenton studies, a current density of 2.8 mA cm^{-2} was maintained ($-0.65 \leq E \leq -0.8$ V) using the synthetic solution (0.07 M TCMTB, 0.03 M Na_2SO_4, and 0.02 M NaCl at pH 3) and using 0.5 mM Fe^{2+}. The presence of Fe^{2+} allows the generation of the homogeneous $^{\cdot}OH$ radical. According to Figure 7, TCMTB degradation is possible given that a decrease in absorbance is observed from 2.2 to 1.5 ($\lambda = 290$ nm) at $Q_v = 5.67$ L min^{-1} in 180 min.

For the anodic oxidation, the BDD anodic potential was maintained between $2.3 \leq E \leq 2.6$ V (a potential range over which BDD($^{\cdot}OH$) is generated) by setting the current density to 6.8 mA cm^{-2}. All of the electrolysis experiments were

Table 1: Current efficiencies for electrochemical generation of H_2O_2 at different volumetric flows ($j = 2.4$ mA cm^{-2}).

Q_v (L min^{-1})	Current efficiency (%)
5.67	24
9.46	32
13.24	51

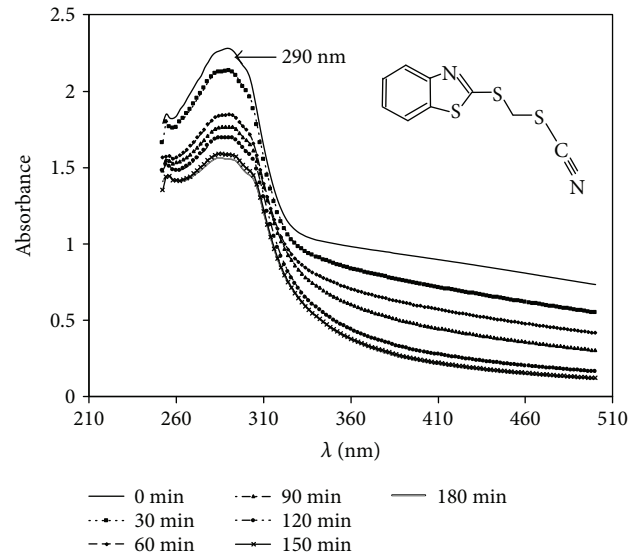

Figure 7: Change in the UV-vis spectra of TCMTB as a function of electrolysis time by the electro-Fenton process in the FM01-LC reactor equipped with an RVC cathode and DSA. Electrolyte: 0.02 M NaCl, 0.03 M Na_2SO_4, and 0.5 mM Fe^{2+} at pH 3. $Q_v = 5.67$ L min^{-1}, 2.8 mA cm^{-2}. $A_{RVC} = 125.95\ cm^2$, $A_{DSA} = 64\ cm^2$.

performed in an undivided FM01-LC reactor, and the electrode potential was controlled over the range in which the desirable electrochemical processes are favored. Figure 8 shows that the turbidity (absorbance) decreases with time in all of the experiments ($\lambda = 290$ nm). For the electro-Fenton process, it is observed that by increasing the feed rate, a higher rate of TCMTB degradation is achieved. As previously discussed, an increase in the flow rate increases the H_2O_2 concentration; thus, the amount of $^{\cdot}OH$ radicals also increases in the bulk solution, favoring the degradation of the TCMTB molecules. A similar phenomenon can be observed in the anodic oxidation process in which an increase in the flow rate also increases the rate of TCMTB degradation. This phenomenon is explained in terms of the effect of increasing the volume flow on the transport of the organic compound from the bulk solution to the electrode surface where radicals are physisorbed BDD($^{\cdot}OH$). A comparison of the EF and AO processes shows that higher percentages of degradation are achieved by anodic oxidation (81%) because the BDD($^{\cdot}OH$) radical is constantly produced on the BDD surface. In EF, the production of homogeneous radicals is limited by the amount of H_2O_2 available for the process because H_2O_2 reacts not only with Fe^{2+} but also with chloride ions, in addition to undergoing its natural decomposition.

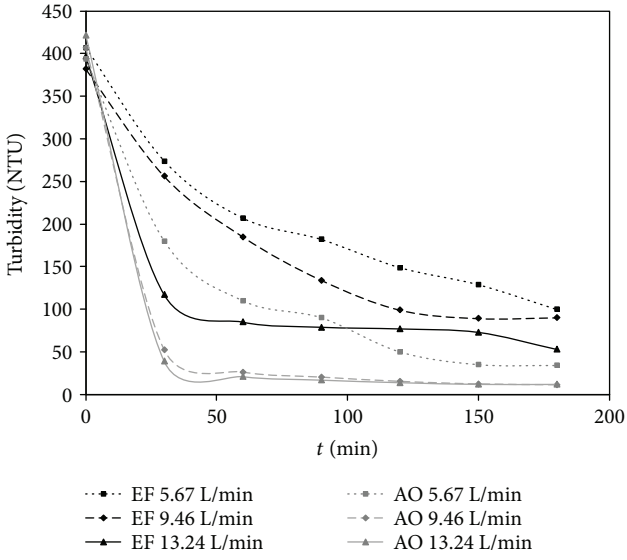

Figure 8: Decrease in turbidity as a function of electrolysis time measured at 290 nm during the EF process in the FM01-LC reactor equipped with an RVC cathode and DSA (at 3 mA cm^{-2}, 0.5 mM Fe^{2+}) and the AO process in the FM01-LC reactor equipped with an stainless steel cathode and BDD anode at 6.8 mA cm^{-2}. $A_{RVC} = 125.95\ cm^2$, $A_{DSA} = 64\ cm^2$, $A_{stainless\ steel} = 64\ cm^2$, and $A_{BDD} = 64\ cm^2$. Electrolyte: 0.07 M TCMTB in 0.02 M NaCl and 0.03 M Na_2SO_4.

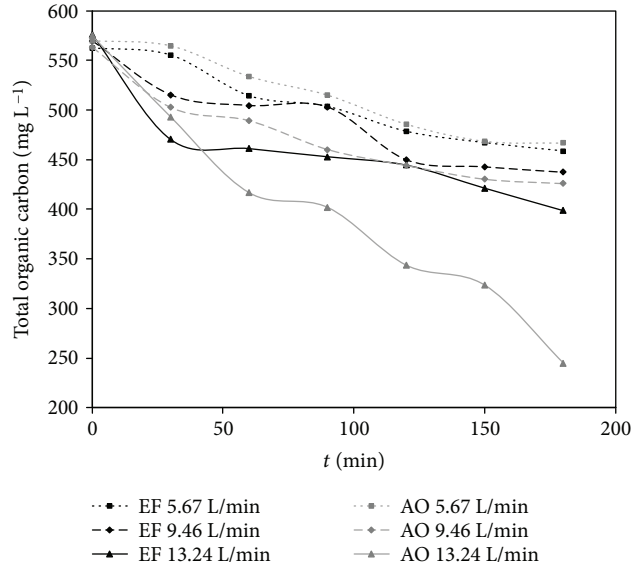

Figure 9: Influence of the volumetric flow rate on TOC removal during the EF and AO processes in the FM01-LC reactor. EF: 2.8 mA cm^{-2}, 0.5 mM Fe^{2+}, $A_{DSA} = 64\ cm^2$, $A_{RVC} = 125.95\ cm^2$. AO: 6.8 mA cm^{-2}, $A_{BDD} = 64\ cm^2$, $A_{stainless\ steel} = 64\ cm^2$. Electrolyte: 0.07 M TCMTB in 0.02 M NaCl and 0.03 M Na_2SO_4.

Although the absorbance for the turbidity values decreases, the TOC values do not decrease at the same rate (Figure 9), indicating that TCMTB is degraded into simpler organic compounds, as has been reported by several authors [10]. It is important to mention that chromatographic studies might help elucidating the differences between the decrease in absorbance and TOC; however, these studies were beyond the scope of this paper. Based on the results obtained here, it is clear that for the anodic oxidation on BDD using a flow rate of 13.24 L min^{-1}, it was possible to achieve up to 57% TCMTB mineralization during the 180 minutes of electrolysis. This achievement was aided by the constant electrogeneration of BDD($^{\cdot}OH$) radicals and the favored transport of TCMTB molecules to the electrode interface.

However, chloride ions affect the percentage of mineralization because they react in a complex mechanism to produce adsorbed chlorine (although weakly sorbed at the electrode surface) and dissolved chlorine, which reacts with water and yields hypochlorous acid, as follows [30]:

$$\begin{aligned} 2Cl^- &\rightarrow Cl_{2,ads} + 2e^- \\ Cl_{2,ads} &\rightarrow Cl_{2,aq} \\ Cl_{2,aq} + H_2O &\rightarrow HClO + H^+ + Cl^- \end{aligned} \quad (9)$$

These reactions could explain why the concentration of chloride ions decreases significantly in the AO experiments, as shown in Table 2. The formed hypochlorous acid could react with hydroxyl radicals to form chlorine dioxide and chlorate [30], thus diminishing the concentration of hydroxyl radicals and preventing higher percentages of mineralization.

$$\begin{aligned} 3^{\cdot}OH + HClO &\rightarrow ClO_2 + 2H_2O \\ 4^{\cdot}OH + HClO &\rightarrow ClO_3{}^- + H^+ + 2H_2O \end{aligned} \quad (10)$$

According to Polcaro et al. [30], for chloride ion concentrations on the BDD anode surface, similar to those in our study, approximately 40% of the current would be used in the formation of chlorine, possibly causing the low current efficiencies observed, which are similar other reports in the literature [23]. However, the removal of chlorides was higher when the volumetric flow was increased, resulting in a major mass transport in the reactor. Moreover, the percentage of mineralization also increased due to the higher mass transport. For the case of sulfates, the concentration did not change in this study.

Table 2 shows that the current efficiency and the mineralization of TCMTB are favored by the increase of Q_v. This increase of current efficiency due to convection flow agrees well with the results reported by Panizza et al. [34]. In addition, the formation of active chlorine species can also aid the TCMTB degradation. A higher Q_v value particularly favors anodic oxidation; thus, better results are obtained than those with the electro-Fenton process. However, the consumption of energy for AO is twice that of EF.

4. Conclusions

Macroelectrolysis studies showed that anodic oxidation produces better percentages of degradation than the electro-Fenton process. This result was most likely due to the

Table 2: Summary of the results obtained during the different experiments.

Experiment	% removal absorbance	% removal TOC	% removal COD	% removal Cl^-	Integral current efficiency, ϕ (%)	Energy consumption (kWh m^{-3})
EF (5.67 L min^{-1})	40	18	42	8	11	0.113
EF (9.46 L min^{-1})	40	23	45	12	13	0.123
EF (13.24 L min^{-1})	47	31	72	12	18	0.116
AO (5.67 L min^{-1})	71	18	32	42	9	0.248
AO (9.46 L min^{-1})	81	24	55	46	12	0.225
AO (13.24 L min^{-1})	81	57	78	52	56	0.225

decreased H_2O_2 concentration caused by different reactions that could occur in the solution in the EF process.

Microelectrolysis studies indicated that the degradation and partial mineralization of TCMTB by anodic oxidation were achieved via hydroxyl radicals formed by the oxidation of water in the BDD electrode under galvanostatic conditions.

Electrolysis in the undivided FM01-LC reactor at different volumetric flows at a current density of 6.8 mA cm^{-2} revealed that the oxidation rate and current efficiency increased as a function of Q_v. This result demonstrates that convection flow favors the influx of TCMTB to the BDD($^{\cdot}$OH) surface, increasing its degradation.

The electrochemical transformation of TCMTB by the electro-Fenton and anodic oxidation processes could be a useful strategy for toxicity reduction.

Nomenclature

BDD: Boron-doped diamond
COD: Chemical oxygen demand (mol L^{-1})
DSA: Dimensionless stable anode
F: Faraday constant (96,485 C mol^{-1})
I: Current applied during electrolysis (A)
j: Current density (A cm^{-2})
Q_v: Volumetric flow (L min^{-1})
RVC: Reticulated vitreous carbon
TCMTB: 2-(Thiocyanomethylthio)-benzothiazole
$TOC_{(0)}$: Initial total organic carbon (mol L^{-1})
$TOC_{(t)}$: Total organic carbon at time t (mol L^{-1})
t: Time of electrolysis (s)
V: Solution volume (L)
ϕ: Current efficiency (%).

Conflicts of Interest

The authors declare that they have no conflicts of interest.

Acknowledgments

The authors are grateful for the SEP-CONACyT grant from the National Council of Science and Technology of Mexico (CONACyT) through the Project no. 240522. Armando Vázquez would like to thank the CONACyT for the doctoral scholarship 217508. The authors also thank the financial support for the publication from SEP-PRODEP. The authors are indebted to Nubia V. Arteaga for laboratory support.

References

[1] D. Pokhrel and T. Viraraghavan, "Treatment of pulp and paper mill wastewater – a review," *Science of The Total Environment*, vol. 333, no. 1-3, pp. 37–58, 2004.

[2] A. Latorre, A. Rigol, S. Lacorte, and D. Barceló, "Organic compounds in paper mill wastewaters," in *The Handbook of Environmental Chemistry*, D. Barceló and A. G. Kostianoy, Eds., vol. 2 of Part O, Springer-Verlag, Berlin Heidelberg, 2005.

[3] K. Tumirah, S. Salamah, A. Rozita, U. Salmiah, and M. A. M. Nasir, "Determination of 2-thiocyanomethylthio benzothiazole (TCMTB) in treated wood and wood preservative using ultraviolet–visible spectrophotometer," *Wood Science and Technology*, vol. 46, no. 6, pp. 1021–1031, 2012.

[4] E. Meneses, M. Arguelho, and J. Alves, "Electroreduction of the antifouling agent TCMTB and its electroanalytical determination in tannery wastewaters," *Talanta*, vol. 67, no. 4, pp. 682–685, 2005.

[5] United States Environmental Protection Agency, "Reregistration eligibility decision for 2-(thiocyanonethylthio) benzothiazole (TCMTB), prevention, pesticides and toxic substances (7510P), EPA739-R-05-003," 2006, October 2017, http://www3.epa.gov/pesticides/chem_search/reg_actions/reregistration/red_PC-035603_1-Aug-06.pdf.

[6] T. Reemtsma, O. Fienh, G. Kalnowski, and M. Jekel, "Microbial transformations and biological effects of fungicide-derived benzothiazoles determined in industrial wastewater," *Environmental Science & Technology*, vol. 29, no. 2, pp. 478–485, 1995.

[7] A. K. Adams and E. M. Warshaw, "Allergic contact dermatitis from mercapto compounds," *Dermatitis*, vol. 17, no. 2, pp. 56–70, 2006.

[8] M. Rajabi, "2-(3,5-Dihydroxyphenyl)-6-hydroxybenzothiazole arrests cell growth and cell cycle and induces apoptosis in breast cancer cell lines," *DNA and Cell Biology*, vol. 31, no. 3, pp. 388–391, 2012.

[9] G. Ginsberg, B. Toal, and T. Kurland, "Benzothiazole toxicity assessment in support of synthetic turf field human health risk assessment," *Journal of Toxicology and Environmental Health, Part A*, vol. 74, no. 17, pp. 1175–1183, 2011.

[10] H. De Wever and H. Verachtert, "Biodegradation and toxicity of benzothiazoles," *Water Research*, vol. 31, no. 11, pp. 2673–2684, 1997.

[11] H. De Wever, H. Verachtert, and P. Besse, "Microbial transformations of 2-substituted benzothiazoles," *Applied Microbiology and Biotechnology*, vol. 57, no. 5-6, pp. 620–625, 2001.

[12] A. Al-Kadasi, A. Idris, K. Saed, and C. T. Guan, "Treatment of textile wastewater by advanced oxidation processes – a review," *Global NEST Journal*, vol. 6, pp. 222–230, 2004,

October 2015, http://journal.gnest.org/sites/default/files/Journal%20Papers/Al-kdasi-222-230.pdf.

[13] H. Särkka, A. Bhatnagar, and M. Sillanppa, "Recent developments of electro-oxidation in water treatment – a review," *Journal of Electroanalytical Chemistry*, vol. 754, pp. 46–56, 2015.

[14] E. Brillas, I. Sirés, and M. Oturan, "Electro-Fenton process and related electrochemical technologies based on Fenton's reaction chemistry," *Chemical Reviews*, vol. 109, no. 12, pp. 6570–6631, 2009.

[15] J. M. Peralta-Hernández, Y. Meas-Vong, F. J. Rodríguez, T. W. Chapman, M. I. Maldonado, and L. A. Godínez, "In situ electrochemical and photo-electrochemical generation of the Fenton reagent: a potentially important new water treatment technology," *Water Research*, vol. 40, no. 9, pp. 1754–1762, 2006.

[16] E. L. Gyenge and C. W. Oloman, "Influence of surfactants on the electro-reduction of oxygen to hydrogen peroxide in acid and alkaline electrolytes," *Journal of Applied Electrochemistry*, vol. 31, no. 2, pp. 233–243, 2001.

[17] P. A. Michaud, M. Panizza, L. Outtara, T. Diaco, G. Foti, and C. H. Comninellis, "Electrochemical oxidation of water on synthetic boron-doped diamond thin film anodes," *Journal of Applied Electrochemistry*, vol. 33, no. 2, pp. 151–154, 2003.

[18] C. A. Martínez-Huitle and E. Brillas, "Decontamination of wastewaters containing synthetic organic dyes by electrochemical methods: a general review," *Applied Catalysis B: Environmental*, vol. 87, no. 3-4, pp. 105–145, 2009.

[19] C. Barrera-Díaz, P. Cañizares, F. J. Fernández, R. Natividad, and M. A. Rodrigo, "Electrochemical advanced oxidation processes: an overview of the current applications to actual industrial effluents," *Journal of the Mexican Chemical Society*, vol. 58, pp. 256–275, 2014.

[20] J. A. Garrido, E. Brillas, P. L. Cabot, F. Centellas, C. Arias, and R. M. Rodríguez, "Mineralization of drugs in aqueous medium by advanced oxidation processes," *Portugaliae Electrochimica Acta*, vol. 25, no. 1, pp. 19–41, 2007.

[21] G. Eisenberg, "Colorimetric determination of hydrogen peroxide," *Industrial and Engineering Chemistry, Analytical Edition*, vol. 15, no. 5, pp. 327-328, 1943.

[22] A. D. Eaton, L. S. Clesceri, E. W. Rice, and A. E. Greenberg, *Standard Methods for the Examination of Water and Wastewater*, APHA, AWWA, & WEF, Washington, USA, 21st edition, 2005.

[23] J. L. Nava, I. Sirés, and E. Brillas, "Electrochemical incineration of indigo. A comparative study between 2D (plate) and 3D (mesh) BDD anodes fitted into a filter-press reactor," *Environmental Science and Pollution Research*, vol. 21, no. 14, pp. 8485–8492, 2014.

[24] A. Vázquez, J. L. Nava, R. Cruz, I. Lázaro, and I. Rodríguez, "The importance of current distribution and cell hydrodynamic analysis for the design of electrocoagulation reactors," *Journal of Chemical Technology and Biotechnology*, vol. 89, no. 2, pp. 220–229, 2014.

[25] J. L. Nava, F. Núñez, and I. González, "Electrochemical incineration of p-cresol and o-cresol in the filter-press-type FM01-LC electrochemical cell using BDD electrodes in sulfate media at pH 0," *Electrochimica Acta*, vol. 52, no. 9, pp. 3229–3235, 2007.

[26] E. Butrón, M. E. Juárez, M. Solis, M. Teutli, I. González, and J. L. Nava, "Electrochemical incineration of indigo textile dye in filter-press-type FM01-LC electrochemical cell using BDD electrodes," *Electrochimica Acta*, vol. 52, no. 24, pp. 6888–6894, 2007.

[27] M. Griffiths, C. Ponce de León, and F. Walsh, "Mass transport in the rectangular channel of a filter-press electrolyzer (the FM01-LC reactor)," *AICHE Journal*, vol. 51, no. 2, pp. 682–687, 2005.

[28] T. Pérez, S. Garcia-Segura, A. El-Ghenymy, J. L. Nava, and E. Brillas, "Solar photoelectro-Fenton degradation of the antibiotic metronidazole using a flow plant with a Pt/air-diffusion cell and a CPC photoreactor," *Electrochimica Acta*, vol. 165, pp. 173–181, 2015.

[29] E. Petrucci, D. Montanaro, and L. Di Palma, "A feasibility study of hydrogen peroxide electrogeneration in seawater for environmental remediation," *Chemical Engineering Transactions*, vol. 28, pp. 91–96, 2012.

[30] A. M. Polcaro, A. Vacca, M. Mascia, S. Palmas, and J. Rodiguez Ruiz, "Electrochemical treatment of waters with BDD anodes: kinetics of the reactions involving chlorides," *Journal of Applied Electrochemistry*, vol. 39, no. 11, pp. 2083–2092, 2009.

[31] A. Alvarez-Gallegos and D. Pletcher, "The removal of low level organics via hydrogen peroxide formed in a reticulated vitreous carbon cathode cell, Part 1. The electrosynthesis of hydrogen peroxide in aqueous acidic solutions," *Electrochimica Acta*, vol. 44, no. 5, pp. 853–861, 1998.

[32] Z. Qiang, J. H. Chang, and C. P. Huang, "Electrochemical generation of hydrogen peroxide from dissolved oxygen in acidic solutions," *Water Research*, vol. 36, no. 1, pp. 85–94, 2002.

[33] K. Cruz-González, O. Torres-López, A. García-León et al., "Determination of optimum operating parameters for Acid Yellow 36 decolorization by electro-Fenton process using BDD cathode," *Chemical Engineering Journal*, vol. 160, no. 1, pp. 199–206, 2010.

[34] M. Panizza, M. Delucchi, and G. Cerisola, "Electrochemical degradation of anionic surfactants," *Journal of Applied Electrochemistry*, vol. 35, no. 4, pp. 357–361, 2005.